

Exciton absorption spectra of RbPb_2Cl_5 and $\text{Rb}_6\text{Pb}_5\text{Cl}_{16}$ thin films

*E.N.Kovalenko*¹, *O.N.Yunakova*², *N.N.Yunakov*²

¹Kharkiv National University of Radio Electronics, 14 Nauky Ave.,
61166 Kharkiv, Ukraine

²V.Karazin Kharkiv National University, 4 Svobody Sq.,
61022 Kharkiv, Ukraine

Received October 23, 2018

The absorption spectra of thin RbPb_2Cl_5 and $\text{Rb}_6\text{Pb}_5\text{Cl}_{16}$ films were studied in the spectral range 2–6 eV and the temperature interval 90–500 K. A correlation was established between the absorption spectra and the crystal structure of the compounds. Excitons in both compounds are localized in a sublattice containing Pb^{2+} ions, and refer to excitons of the intermediate bond. An analysis of the temperature dependence of the half-width of exciton bands establishes a two-dimensional (2D) nature of the excitons in RbPb_2Cl_5 and three-dimensional (3D) in $\text{Rb}_6\text{Pb}_5\text{Cl}_{16}$.

Keywords: Thin RbPb_2Cl_5 and $\text{Rb}_6\text{Pb}_5\text{Cl}_{16}$ films, absorption spectra, crystal structure, exciton.

Исследованы спектры поглощения тонких пленок RbPb_2Cl_5 и $\text{Rb}_6\text{Pb}_5\text{Cl}_{16}$ в спектральном интервале 2–6 эВ и интервале температур 90–500 К. Установлена корреляция между спектрами поглощения и кристаллической структурой соединений. Экситоны в обоих соединениях локализованы в подрешетке, содержащей ионы Pb^{2+} , и относятся к экситонам промежуточной связи. Из анализа температурной зависимости полуширины экситонных полос установлен двухмерный (2D) характер экситонов в RbPb_2Cl_5 и трехмерный (3D) в $\text{Rb}_6\text{Pb}_5\text{Cl}_{16}$.

Екситонні спектри поглинання тонких плівок RbPb_2Cl_5 і $\text{Rb}_6\text{Pb}_5\text{Cl}_{16}$. *О.Н.Коваленко, О.М.Юнакова, М.М.Юнаков.*

Досліджено спектри поглинання тонких плівок RbPb_2Cl_5 та $\text{Rb}_6\text{Pb}_5\text{Cl}_{16}$ у спектральному інтервалі 2–6 еВ і інтервалі температур 90–500 К. Установлено кореляцію між спектрами поглинання і кристалічною структурою сполук. Екситони в обох сполуках локалізовані у підґратці, яка містить іони Pb^{2+} , і відносяться до екситонів проміжного зв'язку. З аналізу температурної залежності напівширини екситонних смуг встановлено двомірний (2D) характер екситонів в RbPb_2Cl_5 і трьохмірний (3D) в $\text{Rb}_6\text{Pb}_5\text{Cl}_{16}$.

1. Introduction

The triple compounds of lead and alkali metal halides crystallize into perovskite-type structures [1–5]. The loose packing in of large radius ions the lattice of lead-halide perovskites provides ample opportunities in crystal composition variations and in ability to change its properties. Such crystals are of practical interest as matrices in

the creation of active laser medium [6–8]. The possibility to vary the width of the forbidden band and embed practically any type of ions into the lattice of lead-halide perovskites makes them promising materials for potential use in galvanic cells of solar batteries, nonlinear optics, and electromagnetic radiation detectors [9, 10].

According to new studies of phase diagram [2] in the RbCl-PbCl_2 system, in addi-

tion to the previously established compounds RbPb_2Cl_5 , RbPbCl_3 and Rb_2PbCl_4 , new compounds $\text{Rb}_6\text{Pb}_5\text{Cl}_{16}$ and Rb_3PbCl_5 have been found. The compound RbPbCl_3 exists only in the temperature range $320^\circ\text{C} - 440^\circ\text{C}$, at $T < 320^\circ\text{C}$ it decomposes into RbPb_2Cl_5 and $\text{Rb}_6\text{Pb}_5\text{Cl}_{16}$. At room temperature, the compounds RbPb_2Cl_5 and $\text{Rb}_6\text{Pb}_5\text{Cl}_{16}$ are stable [2]. RbPb_2Cl_5 crystallizes into a structure of the $\text{NH}_4\text{Pb}_2\text{Cl}_5$ type (spacer group $P2_1/c$) with lattice parameters $a = 8.992 \text{ \AA}$, $b = 7.996 \text{ \AA}$, $c = 12.54 \text{ \AA}$, $\gamma = 90^\circ$, $z = 4$ [1, 2, 5]. The compound $\text{Rb}_6\text{Pb}_5\text{Cl}_{16}$ crystallizes into a tetragonal structure (space group $P4/mbm$) with lattice parameters $a = 11.855 \text{ \AA}$, $c = 11.237 \text{ \AA}$, $z = 4$ [3].

Among compounds formed in the RbCl-PbCl_2 system, RbPb_2Cl_5 crystals are the most studied. Reflection and photoluminescence spectra of RbPb_2Cl_5 crystals were studied in [11–14]. In the recent years luminescence spectra [6, 15] and EPR [16] of RbPb_2Cl_5 crystals doped with rare-earth ions have been actively studied. The exciton absorption spectrum of RbPb_2Cl_5 has not been studied. The reflection spectrum of RbPbCl_3 crystals is given in [14]. Regarding to other compounds of the RbCl-PbCl_2 system, only studies on their crystal structure are known [2, 4].

In this paper the absorption spectra of thin RbPb_2Cl_5 and $\text{Rb}_6\text{Pb}_5\text{Cl}_{16}$ films are studied in the spectral range 2–6 eV and in the temperature range 90–520 K.

2. Experimental

Thin films of RbPb_2Cl_5 and $\text{Rb}_6\text{Pb}_5\text{Cl}_{16}$ were prepared by evaporating a melt of a mixture of pure RbCl and PbCl_2 powders of a stoichiometric molar composition to quartz substrates heated to 373 K, followed by annealing them at a higher temperature of 473 K during two hours. This method was used earlier to obtain thin films of ternary compounds [17–19] and is based on the fact that, as a rule, the melting point of a ternary compound is substantially lower than the melting points of the initial binary components. The melting points of ternary compounds RbPb_2Cl_5 ($T_m = 423^\circ\text{C}$), RbPbCl_3 ($T_m = 440^\circ\text{C}$) and Rb_2PbCl_4 ($T_m = 448^\circ\text{C}$) [2] are noticeably lower than the melting points of the initial components of PbCl_2 ($T_m = 501^\circ\text{C}$) and RbCl ($T_m = 715^\circ\text{C}$) [20]. Due to close values of melting points of the compounds in the RbCl-PbCl_2 system some difficulties arose in obtaining monophase RbPb_2Cl_5 films. Since T_m of RbPb_2Cl_5 is the

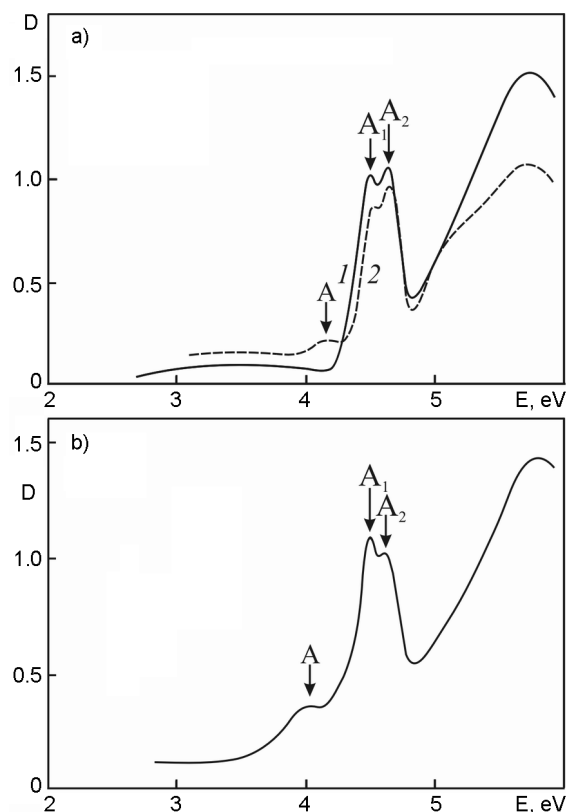


Fig. 1. The absorption spectra of a thin film of RbPb_2Cl_5 (a) $T = 90 \text{ K}$ before annealing (1) and after annealing (2) and a thin film of Rb_3PbCl_5 (b) $T = 90 \text{ K}$ after annealing.

lowest among the compounds of the RbCl-PbCl_2 system, in order to obtain monophasic films the melt of a mixture of stoichiometric composition was evaporated at the lowest possible temperature. The phase composition of the films was monitored from the absorption spectra measured at $T = 90 \text{ K}$. A significant difference in the spectral position of the long-wave exciton bands in PbCl_2 (4.66 eV [21]), RbCl (7.52 eV) and ternary compounds of the RbCl-PbCl_2 system (4.27–4.45 eV [11, 12, 14]) makes it possible to control the absence of an impurity of the initial components in the film using absorption spectra. However, due to the proximity of the spectral positions of the long-wavelength exciton bands in ternary compounds, it is difficult to control the monophasicity of the film by the absorption spectra. But when the film is heated up to $T \geq 473 \text{ K}$, if there is an admixture of compounds of a different molar composition, a band appears at 4.2 eV in the long-wavelength region of the spectrum (Fig. 1). We did not succeed in identifying what compound this band belongs to. The authors of [14] observed a

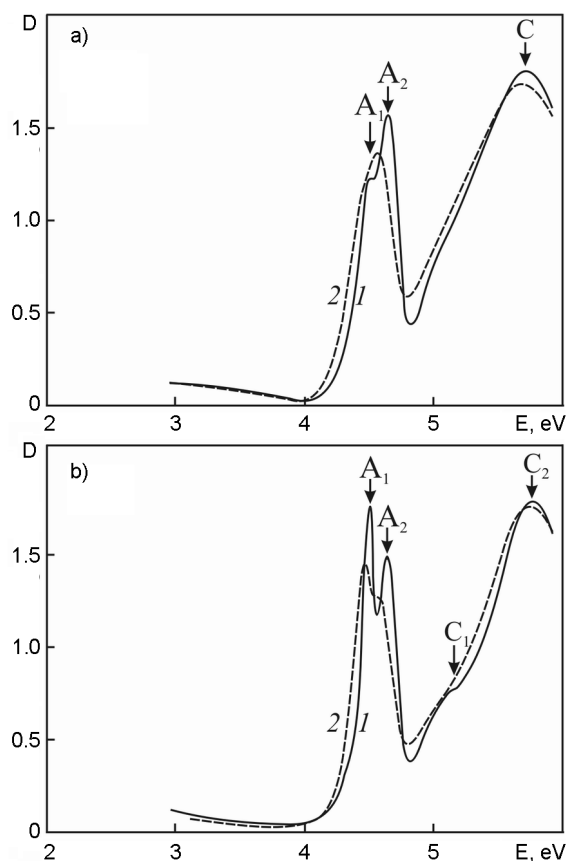


Fig. 2. The absorption spectra of a thin film of RbPb_2Cl_5 (a) ($t = 75$ nm) and a thin film of $\text{Rb}_6\text{Pb}_5\text{Cl}_{16}$ (b) ($t = 75$ nm) at $T = 90$ K (1) and $T = 290$ K (2).

long-wavelength exciton band at 4.27 eV ($T = 77$ K) in the reflection spectrum of single CsPbCl_3 crystal, but according to the phase diagram [2], the compound of such composition does not exist at low temperatures. It should be noted that increase of RbCl concentration in the mixture (molar composition of Rb_3PbCl_5 and Rb_2PbCl_4) leads to the increase of the band intensity at 4.2 eV in the annealed films (Fig. 1b). Eventually we did not succeed in obtaining monophasic Rb_3PbCl_5 and Rb_2PbCl_4 films. The $\text{Rb}_6\text{Pb}_5\text{Cl}_{16}$ phase dominates in the absorption spectra of films of this composition. The authors of [2] note the special stability of the $\text{Rb}_6\text{Pb}_5\text{Cl}_{16}$ compound, which begins to form even when the powders are ground. When the melt of the mixture of the stoichiometric $\text{Rb}_6\text{Pb}_5\text{Cl}_{16}$ composition is evaporated, thin films with a stable absorption spectrum are formed (Fig. 2b). High-temperature annealing does not change the absorption spectrum of $\text{Rb}_6\text{Pb}_5\text{Cl}_{16}$ films.

Consequently, high-temperature annealing contributes to the improvement in films structure and makes it possible to detect the admixture of other ternary compounds phases in RbPb_2Cl_5 films.

The absorption spectra of thin films were measured with a spectrophotometer SF-46 in the spectral range 2–6 eV at $T = 90$ and 290 K. The films with thickness of 75–90 nm were used for the measurement. The absorption spectrum was measured in the temperature range 90–500 K in the region of the long-wave exciton band (3.5–4.9 eV).

The dispersion of the refractive index $n(\lambda)$ in the transparency region of RbPb_2Cl_5 and $\text{Rb}_6\text{Pb}_5\text{Cl}_{16}$ thin films (film thickness 300–600 nm) was determined by the interference method.

To determine the parameters of long-wavelength exciton bands, they were approximation by the method of [22] by a double-oscillator mixed profile, which has having a transitional form from the Lorentz to Gaussian profiles and represents their linear combination. The parameters of the exciton bands (position E_m , half-width Γ and the value of the imaginary part of the permittivity at the maximum of the exciton band $\varepsilon_{2m} \equiv \varepsilon(E_m)$) were chosen to increase accordance of profile with the measured spectra on the long-wavelength side of the bands.

3. Result and discussion

3.1. Absorption spectra of RbPb_2Cl_5 and $\text{Rb}_6\text{Pb}_5\text{Cl}_{16}$ thin films

In the absorption spectrum of a RbPb_2Cl_5 thin film ($T = 90$ K) (Fig. 2a), long-wavelength bands A_1 and A_2 are observed at 4.465 eV and 4.627 eV, respectively, and a broad C band is observed at 5.7 eV. The spectrum of $\text{Rb}_6\text{Pb}_5\text{Cl}_{16}$ thin film (Fig. 2b) is close to the spectrum of RbPb_2Cl_5 by structure and position of absorption bands (see Table). In contrast to RbPb_2Cl_5 , two broad short-wavelength bands C_1 and C_2 are observed in the spectrum of $\text{Rb}_6\text{Pb}_5\text{Cl}_{16}$. When the temperature increases the bands A and C shift to the long-wave region of the spectrum, broaden and weaken due to the exciton-phonon interaction (EPI), which indicates their exciton origin.

After the separation of the A_1 and A_2 bands by a symmetric double-oscillator profile, the width of the band gap for A_2 end the exciton binding energy were determined from the inflection point of the edge of the own absorption band. Their values are $E_{g2} = 4.843, 4.88$ eV and $R_{ex} = E_{g2} - E_{A2} = 0.22,$

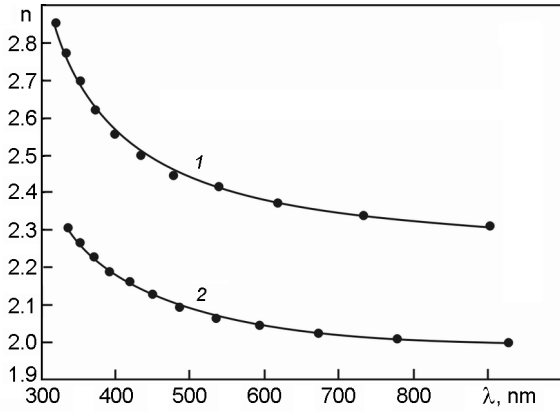


Fig. 3. The spectral dependences of the refractive index $n(\lambda)$ of thin films RbPb_2Cl_5 (1) and $\text{Rb}_6\text{Pb}_5\text{Cl}_{16}$ (2): the points are experi-

0.25 eV in RbPb_2Cl_5 and $\text{Rb}_6\text{Pb}_5\text{Cl}_{16}$, respectively. Assuming that the binding energies of the excitons A_1 and A_2 are equal, we found $E_g = E_{A1} + R_{ex} = 4.68, 4.73$ eV in RbPb_2Cl_5 and $\text{Rb}_6\text{Pb}_5\text{Cl}_{16}$.

The dispersion of the refractive index $n(\lambda)$ in RbPb_2Cl_5 and $\text{Rb}_6\text{Pb}_5\text{Cl}_{16}$ thin films (Fig. 3) in the transparency region is well described by the single-oscillator Wemple model [23]:

$$\varepsilon_1 = n^2 = 1 + \frac{E_d E_0}{E_0^2 - E^2}, \quad (1)$$

where $E = \hbar\omega$, E_0 and E_d are parameters of the single-oscillator model. E_0 determines the spectral position of the effective oscillator associated with the interband optical transitions, $E_0 > E_g$, E_d is the dispersion energy which characterizes the power of the interband transitions.

In the coordinates $(n^2 - 1)^{-1}$ from E^2 the dependence (1) is linear in both compounds. The processing of the experimental data of $n(\lambda)$ in the coordinates $(n^2 - 1)^{-1}$ from E^2 by the method of least squares made it possible to determine from the slope of the straight lines $(E_0 E_d)^{-1} = 6.736 \cdot 10^{-3}, 8.767 \cdot 10^{-3}$ and from the intersection with the ordinate axis $E_0/E_d = 0.244, 0.352$ and $E_0 = 6.018, 6.336$ eV and $E_d = 24.67, 18.0$ eV in RbPb_2Cl_5 and $\text{Rb}_6\text{Pb}_5\text{Cl}_{16}$, respectively. The calculated dependences of $n(\lambda)$ by Eq. 1 (Fig. 3, curve 1) with the found values of E_0 and E_d are in good agreement with the experimental dependences of $n(\lambda)$ (Fig. 3, curve 2). Approximation of the dependences of $n(\lambda)$ to the low-energy limit gives the values of the optical dielectric

constant $\varepsilon_\infty = 1 + E_d/E_0 = 4.1$ and 3.841 in RbPb_2Cl_5 and $\text{Rb}_6\text{Pb}_5\text{Cl}_{16}$, respectively. The obtained values of ε_∞ were used in estimating of radiuses of excitons in the investigated compounds:

$$a_{ex} = a_B \frac{R}{R_{ex} \varepsilon_{eff}}, \quad (2)$$

where $a_B = 0.529 \cdot 10^{-8}$ cm is the Bohr radius, $R = 13.6$ eV is the Rydberg constant, ε_{eff} is the effective dielectric permittivity, $\varepsilon_\infty < \varepsilon_{eff} < \varepsilon_0$, ε_0 is the static permittivity, $R_{ex} = 0.22, 0.25$ eV is the binding energy of excitons in RbPb_2Cl_5 and $\text{Rb}_6\text{Pb}_5\text{Cl}_{16}$ defined above. Since the main contribution to ε_{eff} is determined by the value of ε_∞ in the region of the low-frequency exciton band we used the lower limit ε_{eff} to estimate a_{ex} . The obtained values of $a_{ex} = 7.98 \text{ \AA}$ in RbPb_2Cl_5 and $a_{ex} = 7.49 \text{ \AA}$ in $\text{Rb}_6\text{Pb}_5\text{Cl}_{16}$ indicate intermediate-bond excitons in both compounds.

The absorption spectra of RbPb_2Cl_5 and $\text{Rb}_6\text{Pb}_5\text{Cl}_{16}$ are close to the spectrum of PbCl_2 [21] and the spectra of impurity bands of Pb^{2+} in RbCl [24] by structure and position of the bands. Accordingly, the excitons in these compounds, as well as in PbCl_2 and RbCl:Pb^{2+} , have a cation type and the exciton spectrum is interpreted on the basis of transitions in the Pb^{2+} ion [11, 13, 14]. In contrast to PbCl_2 , two long-wavelength excitonic bands A_1 and A_2 are observed in the spectra of RbPb_2Cl_5 and $\text{Rb}_6\text{Pb}_5\text{Cl}_{16}$, which happens due to the structural features of the crystal lattices of the compounds.

According to [1, 2], there are two non-equivalent positions of lead ions in the crystal structure of RbPb_2Cl_5 . The Pb1 ion [1] is surrounded by 7 Cl ions, which form a distorted tetrahedron with a forked apex (coordination number (CN), respectively, 7). The nearest environment of the second ion Pb2, as well as in PbCl_2 , is a distorted trigonal prism with six chlorine atoms at the apexes and other three ones above the centers of oblong faces, the CN is 9 [1, 2]. In [5], it is proposed to represent the environment of the Pb1 ion in the form of a trigonal prism with six chlorine atoms at the apexes and one above the lateral face, and Pb2 with two Cl atoms above the centers of the side faces with CN equals to 7 and 8, respectively. In PbCl_2 , each Pb ion is surrounded by 9 Cl ions and CN equals to 9. Structural elements

Table. The spectral position of the exciton bands, the band gap E_g and the binding energy of the exciton R_{ex} in the compounds $RbPb_2Cl_5$, $Rb_6Pb_5Cl_{16}$ ($T = 90$ K), $PbCl_2$ and $RbCl:Pb^{2+}$

Compound	E_{mA1} , eV	E_{mA2} , eV	E_{mC1} , eV	E_{mC2} , eV	E_g , eV	R_{ex} , eV
$RbPb_2Cl_5$	4.465	4.627		5.7	4.68	0.22
$Rb_6Pb_5Cl_{16}$	4.475	4.63	5.12	5.7	4.73	0.25
$PbCl_2$ [21]	4.68			5.77	4.86	0.18
$RbCl:Pb^{2+}$ [24]	4.582		5.85	6.192		

with Pb1 and Pb2 ions form layers separated by layers containing Rb ions [1, 2, 5]. The layered structure of the $RbPb_2Cl_5$ crystal lattice determines the two-dimensional character of the excitons in the compound, which will be shown below.

The shorter wavelength A_2 band in $RbPb_2Cl_5$ is close to the long-wave exciton band in $PbCl_2$ (Table), and corresponds to the transition in the Pb2 ion with a large value of the CN. The A_1 band is associated with a transition in the Pb1 ion with a smaller value of the CN, which determines its longer wavelength spectral position.

Despite the higher symmetry, the crystal structure of $Rb_6Pb_5Cl_{16}$ is rather complicated. There are three different coordination polyhedrons for Rb ions and two for Pb ions [4]. The Pb(1) ion (in the notation of [4]) has a quadratic antiprismatic coordination with a CN of 9, another lead ion (in the notation of [4]) Pb/Rb, a site partially substituted by Rb) is surrounded by 8 chlorine atoms in a distorted polyhedron (CN = 8). The presence of two positions of Pb ions with different CN in the crystal structure of $Rb_6Pb_5Cl_{16}$ causes two long-wave exciton bands A_1 and A_2 in the absorption spectrum of the compound.

In $Rb_6Pb_5Cl_{16}$ polyhedra with Rb(1), Pb(1) and Pb/Rb alternate with polyhedra containing Rb(2) and Rb(3), forming a close packing [4]. The tetragonal $Rb_6Pb_5Cl_{16}$ crystal is three-dimensional and, the excitons in this compound have a 3D characters will be shown below.

It should be noted that the narrower excitonic bands A_1 and A_2 in the spectrum of $Rb_6Pb_5Cl_{16}$ ($\Gamma_1 = 0.13$ eV and $\Gamma_2 = 0.13$ eV, $T = 90$ K) in comparison to $RbPb_2Cl_5$ ($\Gamma_1 = 0.18$ eV and $\Gamma_2 = 0.195$ eV, $T = 90$ K) indicate a larger structural perfection of the films of the first compound. Therefore, we observe two exciton bands C_1 and C_2 in the spectrum of $Rb_6Pb_5Cl_{16}$, corresponding to transitions in Pb ions with different CN. In $RbPb_2Cl_5$, it seems that the C_1 and C_2 bands merge into a wide exciton band C .

In $Rb_6Pb_5Cl_{16}$, the long-wavelength exciton band A_1 is associated with the transition in the Pb ion with the CN = 8, in $RbPb_2Cl_5$ with the CN = 7, which causes a large ionicity of the first compound and a slightly shifted edge of absorption to the short-wave region (Fig. 2, Table).

3.2. Temperature dependence of the parameters of long-wavelength exciton bands in $RbPb_2Cl_5$ and $Rb_6Pb_5Cl_{16}$ thin films

In the region of long-wave exciton bands A_1 and A_2 (3.5–4.9 eV), the absorption spectra of $RbPb_2Cl_5$ and $Rb_6Pb_5Cl_{16}$ thin films of were measured in the temperature range 90–500 K.

When the temperature increases the bands A_1 and A_2 in $RbPb_2Cl_5$ linearly shift to the long-wavelength region of the spectrum with $dE_{m1}/dT = -(3.27 \pm 0.02) \cdot 10^{-4}$ eV/K and $dE_{m2}/dT = -(3.2 \pm 0.02) \cdot 10^{-4}$ eV/K, in $Rb_6Pb_5Cl_{16}$ with $dE_{m1}/dT = -(2.12 \pm 0.04) \cdot 10^{-4}$ eV/K and $dE_{m2}/dT = -(2.08 \pm 0.04) \cdot 10^{-4}$ eV/K, (Fig. 4a, 4c). In order of magnitude such a shift is characteristic for ionic crystals, to which the investigated compounds belong.

For ionic crystals, the preferential interaction of excitons with longitudinal optical (LO) phonons is typical, and the largest temperature variations of the parameters of the exciton bands occur at $\hbar\omega_{LO} \leq kT$ accordingly. When the temperature increases the half-width of the exciton bands A_1 and A_2 in both compounds increases nonlinearly (Fig. 4b, 4d). The broadening of the exciton band due to the exciton-phonon interaction $\Gamma(T)$ for excitons of various dimensions d ($d = 1, 2, 3$), according to the theory of [25], is defined as

$$\Gamma(T) \approx \left[\frac{\pi D^2}{\gamma(d/2)(2\pi B)^{d/2}} \right]^{2/4-d}, \quad (3)$$

where $\gamma(d/2)$ is the gamma function depending on d , B is the width of the exciton band and

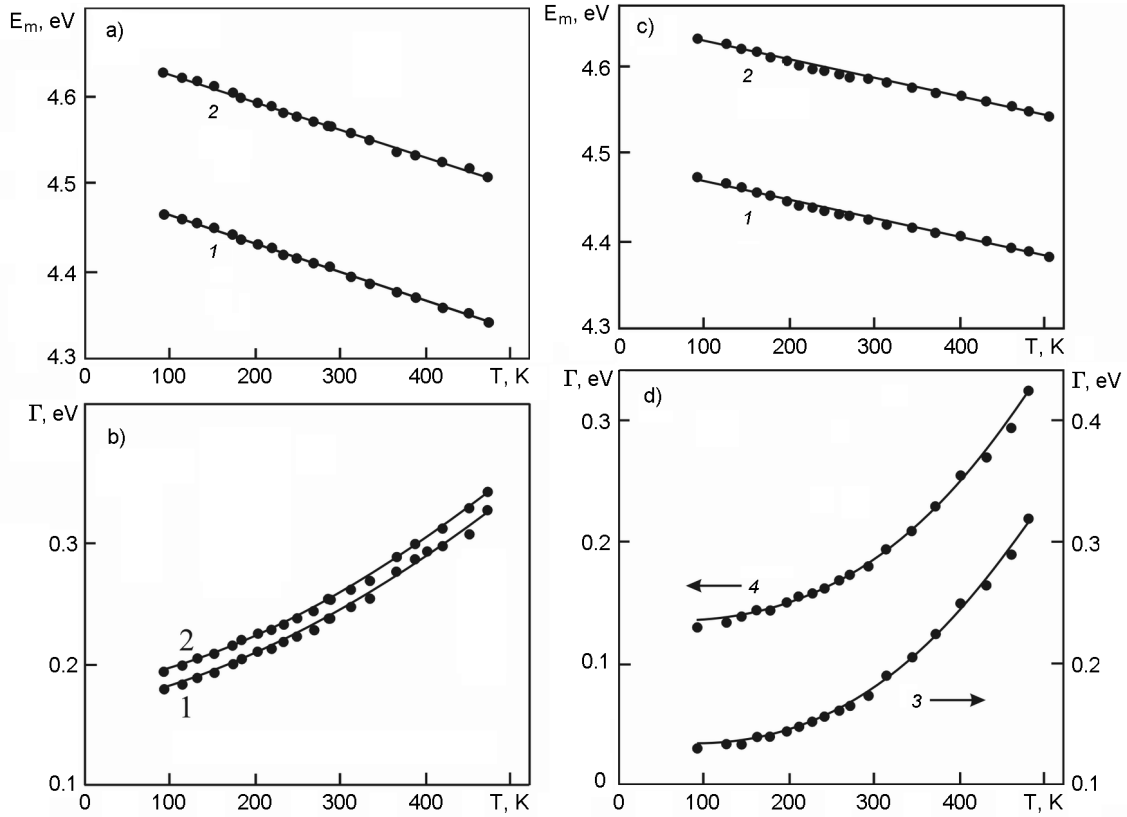


Fig. 4. The temperature dependences of the spectral position of $E_m(T)$ (a) and the half-width $\Gamma(T)$ (b) of long-wavelength excitonic bands A_1 (1) and A_2 (2) in a thin film of RbPb_2Cl_5 and $E_m(T)$ (c) and $\Gamma(T)$ (d) bands A_1 (1) and A_2 (2) in a thin film of $\text{Rb}_6\text{Pb}_5\text{Cl}_{16}$. In Fig. 4b, 4d: points — experiment, solid curve — calculation using formulas 4, 5 and 4,6.

$D^2 = 0.5 \cdot C^2 \hbar\omega_{LO} \text{cth}(\hbar\omega_{LO}/2kT)$, $\hbar\omega_{LO} = 24.8$ meV is the energy of LO phonons in RbPb_2Cl_5 and $\text{Rb}_6\text{Pb}_5\text{Cl}_{16}$ [13], $C^2/2$ is the lattice relaxation energy when exciting an exciton. It is also necessary to take into account the contribution of the residual broadening $\Gamma(0)$ due to lattice defects to the total half-width of the exciton band Γ . The shape of the exciton bands A_1 and A_2 at low temperatures is close to Gaussian, and at high temperatures it is completely Gaussian. In the case of a Gaussian contour of the exciton band, the total half-width Γ can be represented as

$$\Gamma = [\Gamma^2(0) + \Gamma^2(T)]^{1/2}, \tag{4}$$

where $\Gamma(T)$ is represented by the formula (3) with an unknown factor Q independent on T . Processing of the experimental dependences $\Gamma_1(T)$ and $\Gamma_2(T)$ by formula 3 for different d gives the best agreement of calculation with experiment in RbPb_2Cl_5 at $d = 2$, in $\text{Rb}_6\text{Pb}_5\text{Cl}_{16}$ at $d = 3$. For $d = 2$

$$\Gamma(T) = Q \text{cth}(\hbar\omega_{LO}/2kT), \tag{5}$$

and the dependences $\Gamma_1(T)$ and $\Gamma_2(T)$ in RbPb_2Cl_5 in the coordinates Γ^2 from $\text{cth}^2(\hbar\omega_{LO}/2kT)$ are linear. The processing of these dependences by the method of least squares gives the values of $\Gamma_1(0) = 0.16 \pm 0.002$ eV, $\Gamma_2(0) = 0.17 \pm 0.001$ eV and $Q_1 = 0.084 \pm 0.0007$ eV, $Q_2 = 0.087 \pm 0.0005$ eV. The calculated temperature dependences of $\Gamma_1(T)$ and $\Gamma_2(T)$ with the found values of $\Gamma_{1,2}(0)$ and $Q_{1,2}$ according to formulas 4,5 are in good agreement with the experimental ones (Fig. 4b).

In $\text{Rb}_6\text{Pb}_5\text{Cl}_{16}$, the best agreement between the calculated dependences of $\Gamma_1(T)$ and $\Gamma_2(T)$ with experimental ones is reached at $d = 3$. In this case

$$\Gamma(T) = Q \text{cth}^2(\hbar\omega_{LO}/2kT). \tag{6}$$

The least-squares processing of the dependences $\Gamma_1(T)$ and $\Gamma_2(T)$ linear in the co-

ordinates Γ^2 from $\text{cth}^4(\hbar\omega_{LO}/2kT)$ gives the values $\Gamma_1(0) = 0.13 \pm 0.002$ eV, $\Gamma_2(0) = 0.14 \pm 0.001$ eV and $Q_1 = 0.025 \pm 0.0001$ eV, $Q_2 = 0.025 \pm 0.0002$ eV. The calculated dependences $\Gamma_1(T)$ and $\Gamma_2(T)$ from formulas (4), (6) and the found values of $\Gamma_{1,2}(0)$ and $Q_{1,2}$ in $\text{Rb}_6\text{Pb}_5\text{Cl}_{16}$ agree well with the experimental ones (Fig. 4d).

Analysis of the temperature dependences of $\Gamma_1(T)$ and $\Gamma_2(T)$ proves the two-dimensional (2D) type of the excitons in RbPb_2Cl_5 and the three-dimensional (3D) in $\text{Rb}_6\text{Pb}_5\text{Cl}_{16}$, which agrees with the structure of the crystal lattices of the compounds.

4. Conclusions

The absorption spectra of thin RbPb_2Cl_5 and $\text{Rb}_6\text{Pb}_5\text{Cl}_{16}$ films were studied in the spectral range 2–6 eV and the temperature interval 90–500 K. The binding energy of excitons and the width of the forbidden band in both compounds are determined.

The excitons in both compounds, like in PbCl_2 , are cationic in nature and refer to excitons of the intermediate bond. In the cationic exciton model, the absorption spectrum of the investigated compounds, like PbCl_2 is interpreted on the basis of transitions in the Pb ion. The presence of two positions of Pb ions with different CN in the crystal structure of both compounds causes the appearance of two long-wave excitonic bands A_1 and A_2 and two bands C_1 and C_2 in the spectra of $\text{Rb}_6\text{Pb}_5\text{Cl}_{16}$.

The two-dimensional (2D) nature of the excitons in RbPb_2Cl_5 and three-dimensional (3D) in $\text{Rb}_6\text{Pb}_5\text{Cl}_{16}$ is established from the analysis of the temperature dependences of $\Gamma_1(T)$ and $\Gamma_2(T)$ of long-wave exciton bands A_1 and A_2 , which agrees with the structure of the crystal lattices of the compounds.

References

1. K.Nitsch, M.Dusek, M.Niki et al., *Prog. Cryst. Growth and Charact.*, **30**, 1 (1995).
2. H.Monzel, M.Schramm, K.Stowe, H.P.Beck, *Z. Anorg. Allgem. Chem.*, **626**, 408 (2000).
3. H.P.Beck, M.Schramm, R.Haberkorn, *Z. Anorg. Allgem. Chem.*, **624**, 393 (1998).
4. H.P.Beck, H.Monzel, R.Haberkorn et al., *Z. Anorg. Allgem. Chem.*, **625**, 1998 (1999).
5. A.A.Merkulov, L.I.Isaenko, V.M.Pashkov et al., *J. Struct. Chem.*, **46**, 103 (2005).
6. A.Okhrimchuk, V.Mezentsev, N.Lichkova, *Optics & Laser Technology*, **92**, 80 (2017).
7. P.A.Tanner, G.Jia, B.-M.Cheng, M.G.Brik, *Phys. Stat. Sol. B*, **249**, 581 (2012).
8. A.M.Tkachuk, S.E.Ivanova, M.F.Joubert et al., *J. Luminescence*, **125**, 271 (2007).
9. L.K.Ono, E.J.Juarez-Perez, Y.Qi, *ACS Appl. Mater. Interfaces*, **9**, 30197 (2017).
10. Y.Hu, Y.Guo, Y.Wang, Z.Chen, *J. Mater. Res.*, **32**, 3992 (2017).
11. I.N.Ogorodnikov, N.S.Bastrikova, V.A.Pustovarov, L.I.Isaenko, *J. Opt. Soc. Am. B*, **31**, 1935 (2014).
12. M.Niki, K.Nitsch, K.Polak, *Phys. Stat. Solidi (b)*, **166**, 511 (1991).
13. V.A.Pustovarov, I.N.Ogorodnikov, N.S.Bastrikova et al., *Opt. and Spectr.*, **101**, 247 (2006).
14. S.V.Myagkota, A.S.Voloshinovskii, I.V.Stefanskii et al., *Radiat. Meas.*, **29(3-4)**, 273 (1998).
15. A.Okhrimchuk, L.Butvina, E.Dianov et al., *J. Opt. Soc. Am. B*, **24**, 2690 (2007).
16. V.A.Vazhenin, A.P.Potapov, A.N.Ivachev et al., *Solid State Phys.*, **54**, 1168 (2012).
17. O.N.Yunakova, V.K.Miloslavsky, E.N.Kovalenko, V.V.Kovalenko, *Low Temperature Physics*, **41**, 830 (2015).
18. O.N.Yunakova, V.K.Miloslavskiy, E.N.Kovalenko, *Functional Materials*, **20**, 59 (2013).
19. O.N.Yunakova, V.K.Miloslavsky, E.N.Kovalenko, E.V.Ksenofontova, *Low Temperature Physics*, **38**, 1191 (2012).
20. I.T.Goronovsky, Yu.P.Nazarenko, E.F.Nekryach, *Quick Reference Book on Chemistry*, Naukova Dumka, Kiev (1987).
21. M.Fujita, M.Itoh, Y.Bokomoto et al., *Phys. Rev. B*, **61**, 15731 (2000).
22. O.N.Yunakova, V.K.Miloslavsky, E.N.Kovalenko, *Opt. and Spectr.*, **104**, 631 (2008).
23. K.Schmitt, *Phys. Stat. solidi (b)*, **113**, 559 (1982).
24. M.Schreiber, Y.Toyazawa, *J. Phys. Soc. Japan*, **51**, 1528 (1982).